

## PRECISION EPHEMERIDES FOR GRAVITATIONAL-WAVE SEARCHES: I. SCO X-1

DUNCAN K. GALLOWAY<sup>1,2,3,4</sup>, SAMMANANI PREMACHANDRA<sup>2</sup>, DANNY STEEGHS<sup>5</sup>, TOM MARSH<sup>5</sup>, JORGE CASARES<sup>6,7</sup>,  
AND RÉMON CORNELISSE<sup>6,7</sup><sup>1</sup>Monash Centre for Astrophysics, Monash University, VIC 3800, Australia; <sup>5</sup>Department of Physics, Astronomy and Astrophysics group, University of Warwick, CV4 7AL, Coventry, UK; <sup>6</sup>Instituto de Astrofísica, E-38205, La Laguna, Tenerife, Spain*Accepted by ApJ*

## ABSTRACT

Rapidly-rotating neutron stars are the only candidates for persistent high-frequency gravitational wave emission, for which a targeted search can be performed based on the spin period measured from electromagnetic (e.g. radio and X-ray) observations. The principal factor determining the sensitivity of such searches is the measurement precision of the physical parameters of the system. Neutron stars in X-ray binaries present additional computational demands for searches due to the uncertainty in the binary parameters. We present the results of a pilot study with the goal of improving the measurement precision of binary orbital parameters for candidate gravitational wave sources. We observed the optical counterpart of Sco X-1 in 2011 June with the William Herschel Telescope, and also made use of Very Large Telescope observations in 2011, to provide an additional epoch of radial-velocity measurements to earlier measurements in 1999. From a circular orbit fit to the combined dataset, we obtained an improvement of a factor of two in the orbital period precision, and a factor of 2.5 in the epoch of inferior conjunction  $T_0$ . While the new orbital period is consistent with the previous value of Gottlieb et al. (1975), the new  $T_0$  (and the amplitude of variation of the Bowen line velocities) exhibited a significant shift, which we attribute to variations in the emission geometry with epoch. We propagate the uncertainties on these parameters through to the expected Advanced LIGO & VIRGO detector network observation epochs, and quantify the improvement obtained with additional optical observations.

*Subject headings:* ephemerides — gravitational waves — stars: neutron — techniques: radial velocities — X-rays: binaries — X-rays: individual(Sco X-1)

## 1. INTRODUCTION

Neutron stars orbiting low-mass stellar companions typically rotate many hundreds of times every second (e.g. Chakrabarty et al. 2003), because the mass transferred within these low-mass X-ray binary (LMXB) systems over their long ( $\sim 10^9$  year) lifetimes causes the neutron star to spin up. These extreme objects must be highly spherical due to the intense gravitational field; the equivalent of the tallest mountain possible on Earth might be only a few centimetres high on a neutron star. However, there are number of physical processes thought to permit slight ( $\sim 10^{-6}$ ) deviations from axisymmetry, for example from a temperature asymmetry arising from a non-aligned magnetic field (Bildsten 1998). A quadrupole mass moment will lead to gravitational wave emission at twice the neutron star spin frequency,  $\nu_s$ . Assuming a balance between spin-up torques and angular momentum losses from gravitational wave emission, the expected gravitational wave strength at the Earth from a distant source is proportional to the accretion rate (measured locally as the incident X-ray flux,  $F_X$ ) and the spin

frequency:

$$h_0 \approx 4 \times 10^{-27} \left( \frac{F_X}{10^{-8} \text{ erg cm}^{-2} \text{ s}^{-1}} \right)^{1/2} \times \left( \frac{300 \text{ Hz}}{\nu_s} \right)^{1/2} \quad (1)$$

where  $h_0 = \Delta L/L$  is the “strain”, i.e. the fractional change in length of (for example) an interferometer arm, and  $\nu_s$  is the neutron star spin frequency. The best targets for searches for GW then, are the brightest sources with the lowest spin frequencies. Unfortunately, the brightest neutron-star binaries, the so-called “Z-sources” (after their characteristic X-ray spectral behaviour; Hasinger & van der Klis 1989), are also those for which the spin periods are unknown. Spin measurements in about 20% of known LMXBs have been made by detecting various types of transient X-ray intensity pulsations (e.g. Watts 2012); however, none of these phenomena have yet been detected in the brightest class of sources.

The principal difficulty in searching for the gravitational waves emitted by neutron stars is the lack of precise knowledge about the neutron star spin. This problem is compounded for sources in LMXBs where one must also correct for the position and velocity of the neutron star in its binary orbit (Watts et al. 2008). Without precise knowledge of the spin frequency and orbital parameters, a search may still be carried out, but an observational “penalty” must be paid. Effectively, the signal

Duncan.Galloway@monash.edu

<sup>2</sup> also School of Physics, Monash University, VIC 3800, Australia<sup>3</sup> also School of Mathematical Sciences, Monash University, VIC 3800, Australia<sup>4</sup> ARC Future Fellow<sup>7</sup> also Departamento de Astrofísica, Universidad de La Laguna, E-38205, La Laguna, Tenerife, Spain

must be proportionately stronger, compared to a source where the parameters are known more precisely, to reach the same level of confidence for a detection.

Contemporary (published) searches for the periodic gravitational wave emission of these objects have adopted one of two techniques. The first is a “matched filtering” approach which involves comparing the observed signal from the interferometer with a model signal coherently over some time interval  $T_{\text{obs}}$  (e.g. Abbott 2007). This is currently the most sensitive method known (in the limit of infinite computational power) and therefore the method of choice when not computationally bound by a prohibitively large parameter space. For LMXB sources, generally there is some large degree of uncertainty in the model parameters, demanding the requirement for multiple models (“templates” or “filters” in the GW search parlance). The second method is an example of a semi-coherent approach, in this case involving the cross-correlation of the outputs of two or more detectors coherently over short intervals, the products of which are combined incoherently over the length of the observation (Dhurandhar et al. 2008; Chung et al. 2011). Other variations on the semi-coherent theme are in development at present but as is the case for all of them, sensitivity is sacrificed for computational feasibility and therefore the reason such approaches are used is entirely due to the large uncertainties in the system parameters.

Sco X-1, the brightest of the known LMXBs, has already been the subject of two searches with data from the initial LIGO detectors. In the first of these analyses (Abbott 2007), a fully coherent search using data from the 2-mo second science run (S2), the uncertainties in the orbital parameters and the unknown spin period principally determined the search sensitivity, via the maximum duration (6 hr) of data that could be searched coherently with the available computer power. This is a tiny fraction of the available observing time. The second analysis, a semi-coherent radiometer method, is a novel non-optimal approach applied to Sco X-1 at a significant cost in sensitivity because of the large uncertainty in the source parameters (Abbott et al. 2007).

It follows that if the system parameters were known precisely enough that the deviation between the model and the target signal is small (less than one cycle) over  $T_{\text{obs}}$ , a fully coherent matched filter approach can be used and optimal sensitivity can be achieved.

Sco X-1 is also one of the rare cases among the low-mass X-ray binaries where the system is relatively unobscured and is bright in the optical band ( $V \approx 12.5$ ). The orbital period is well known from 89 years of photometry (Gottlieb et al. 1975). Previous high-resolution spectroscopic studies of Sco X-1 led to the discovery of the first tracer of the unseen mass donor star (Steehghs & Casares 2002; hereafter SC02). These studies revealed emission components from the irradiated low mass donor star, principally within the Bowen fluorescence lines near 4640 Å.

Despite the relatively high precision of the orbital parameters for Sco X-1, the current ephemeris has been derived from data obtained in 1999 or earlier, and thus will not have adequate precision to guide gravitational wave searches in the A-LIGO era. In order to cover the possible parameter space in the search, the orbital parameter

uncertainties *at the time of the gravitational wave observation* must be known. This can be estimated from previous measurements, given sufficient information, such as the covariance matrix for the fit by which the orbital parameters are measured; but this information is not currently available.

Here we present initial results from a pilot program of optical observations of the stellar counterparts to X-ray bright accreting neutron stars, in order to improve the precision of the binary parameters. These measurements will allow sensitivity improvements for future gravitational wave searches, and will also facilitate pulsation searches with the extensive X-ray timing data from NASA’s *Rossi X-ray Timing Explorer (RXTE)*, to measure the spin frequency.

## 2. OBSERVATIONS

We summarise the source data for this paper in Table 1. We observed Sco X-1 for a second epoch on the nights of 2011 June 16–18, using the Intermediate dispersion Spectrograph and Imaging System (ISIS), at the Cassegrain focus of the 4.2m William Herchel Telescope (WHT), La Palma. ISIS is a high-efficiency double beam spectrograph, providing medium resolution spectra with dispersion in the range 8–120 Å/mm. For the new observations, we adopted the H2400B grating on the blue arm in order to achieve a spectral resolution of 0.32 Å imaged with the 2048 × 4096 pixel EEV CCD detector. We used a 1.0” slit and obtained spectra covering a wavelength range of 4400–5000 Å at 0.11 Å per pixel. At the central wavelength of 4700 Å, a resolution element spans 20 km s<sup>−1</sup>. A total of 157 spectra were obtained in 300-s exposures over three consecutive nights, covering 75% of the 18.9 hr orbital cycle.

We reanalysed the spectra reported by SC02, also obtained with ISIS on the WHT. The R1200B grating was used for those observations, covering the wavelength range 4150–5050 Å at 0.45 Å per pixel. The spectra were recorded using a 2048 × 4096 pixel EEV CCD detector; a 1”/2 slit gave a spectral resolution of 0.84 Å, corresponding to 55 km s<sup>−1</sup> at the central wavelength of 4601 Å. A total of 137 spectra were obtained over the nights of 1999 June 28–30, covering 75% of the orbital cycle. For full details of those observations, refer to SC02.

We further observed Sco X-1 in a series of observations with the Ultraviolet and Visual Echelle Spectrograph (UVES), on the European Southern Observatory (ESO) Very Large Telescope (VLT) between 29 May–23 August 2011 (programme 087.D-0278). UVES is a two-arm cross dispersed echelle spectrograph, providing a resolving power up to 80,000 in the blue arm (Dekker et al. 2000). A total of 44 exposures lasting 720 s each were made using a 2048 × 4096 pixel EEV CCD detector, covering the wavelength range 3000–5000 Å at 0.0294 Å/pixel. A 1 arcsec slit was used, giving spectral resolution of 0.1 Å (8 km s<sup>−1</sup>).

The WHT spectral data were reduced using a series of PAMELA<sup>5</sup> routines. Raw frames were first debiased using a median bias frame calculated from combining 20–25 individual bias exposures. Flat field correction was achieved using median of  $\approx 40$  Tungsten exposures con-

<sup>5</sup> <http://deneb.astro.warwick.ac.uk/phsaap/software>

structed each night. The frames were then flat fielded, this corrected for pixel-to-pixel variations in responsivity in order to normalize the background counts and help remove systematically hot or dead pixels. CuNe and CuAr arc images were observed for the purpose of wavelength calibration. Arc images were taken regularly throughout each night, with wavelength solutions for each source spectrum interpolated from the nearest arcs before and after. The long slit was rotated to accommodate a nearby comparison star in order to monitor slit-losses.

Sky subtraction was achieved by selecting the sky and object regions and fitting polynomials in order to estimate the sky under the object. The target and comparison star spectra were then optimally extracted for each exposure. Finally, a wide slit exposure of the flux standards BD284211 and MHZ44 (Oke 1990) was used to perform flux calibration using MOLLY<sup>1</sup> data analysis package.

UVES echelle spectra were reduced using the pipeline provided by ESO<sup>6</sup>. After reaching the last stage of data reduction, we transformed the spectra using IRAF into a format that can be read by the MOLLY software package.

Following SC02, we analysed the narrow emission lines arising from individual Bowen transitions, which are superimposed on a broader emission component centred around 4640 Å. The strongest Bowen components are the C III component at 4647.4 Å and the two N III components at 4634.1 and 4640.6 Å. These Bowen components move in phase with each other and move in antiphase with the He II emission (SC02).

All the individual 338 spectra were normalized to the continuum. Following SC02, we fitted a model consisting of a broad underlying Gaussian component and three narrow components, with central wavelengths for the lines having a common offset corresponding to the line-of-sight radial velocity. We fixed the widths of the line components to values used in SC02; the full-width at half maximum (FWHM) was fixed to 1250 km s<sup>-1</sup> for the broad component and 75 km s<sup>-1</sup> for the narrow components. The model normalisation for each line was free to vary independently.

We also used *V*-magnitude aperture photometry of Sco X-1 made for the All-Sky Automated Survey (ASAS; Pojmanski & Maciejewski 2004). This program provides continuous monitoring of the whole sky with automated instruments located in Chile and Hawaii. Each instrument consists of a wide-field (9° × 9°) camera equipped with an f200/2.8 telephoto lens; photometric magnitudes are determined with a range of apertures (2–6 pixels in diameter) for all stars to a limiting magnitude of *V* ≈ 14. We obtained a total of 640 measurements of Sco X-1 between 2001 and 2009. The mean uncertainty was 0.047 magnitudes.

### 3. ANALYSIS AND RESULTS

#### 3.1. Photometric variations

In order to identify the correct orbital period from the candidates of Gottlieb et al. (1975) and Vanderlinde et al. (2003), we first performed a periodicity search of the *V*-band photometry from ASAS. We plot the *V*-magnitude for the optical counterpart to Sco X-1 in Fig.

<sup>6</sup> <http://www.eso.org/sci/software/pipelines>

**Table 1**  
Observations of Sco X-1, 1999–2011

Instrument/source	Date	<i>n</i> <sub>obs</sub>	Ref.
ISIS/WHT	1999 Jun 28–30	137	[1]
ASAS <sup>a</sup>	2001 Jan 22–2009 Oct 5	567 <sup>b</sup>	[2]
UVES/VLT	2011 May 29–Aug 23	44	[3]
ISIS/WHT	2011 Jul 16–18	157	[3]

**References.** — 1. SC02, 2. Pojmanski & Maciejewski (2004), 3. this paper

<sup>a</sup> <http://www.astrouw.edu.pl/asas>

<sup>b</sup> Grade A & B measurements, retained from 640 total measurements

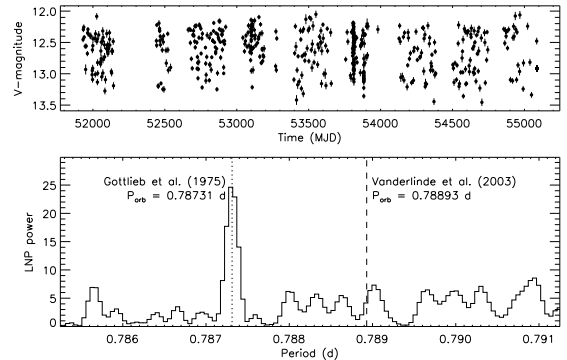


**Figure 1.** *V*-band photometry of Sco X-1 from the All-Sky Automated Survey (ASAS). The top panel shows the raw data, consisting of 567 grade A & B measurements between 2001 and 2009. The bottom panel shows the Lomb-normalised periodogram of the data. The candidate orbital period is shown as the dotted line (Gottlieb et al. 1975) and the alias from the *RXTE*/ASM data is shown as the dashed line (Vanderlinde et al. 2003). Note the excess of power at 0.787313 d; the estimated significance is  $1.7 \times 10^{-7}$ , equivalent to  $5.1\sigma$ .

1 (*top panel*). We adopted the magnitudes measured with the smallest aperture (2 micron); our results were only weakly sensitive to the choice of aperture. The mean intensity was  $V = 12.7 \pm 0.3$ .

We calculated a Lomb-normalised periodogram in the frequency range  $10^{-6}$ – $1.34$  d<sup>-1</sup>. The mean power thus measured was 2.95, with standard deviation 2.57. The maximum power in this range was 24.6, at a period of 0.78730 d (Fig. 1, *bottom panel*), where the resolution was approximately  $5 \times 10^{-5}$  d. This period is in good agreement with the value of Gottlieb et al. (1975); in contrast, the maximum power measured within 0.001 d of the alias value of 0.78893 d was 7.3. This value is consistent at the  $1.7\sigma$  level with the full-frequency range distribution of powers.

Recently a similar analysis was reported adopting the same data (Hynes & Britt 2012). Our results are identical to that work. Hynes & Britt (2012) derived a period of 0.787313(15) d, which is consistent with the Gottlieb et al. (1975) period (but not the value of Vanderlinde et al. 2003), confirming the former value as the orbital period for Sco X-1. The epoch of minimum light for the ASAS data is  $T_{\min}(\text{HJD}) = 2453510.329(17)$ , consistent to within the uncertainties with the projected Gottlieb et al. (1975) ephemeris. Below we present additional analysis leading to further refinement of these orbital parameters.

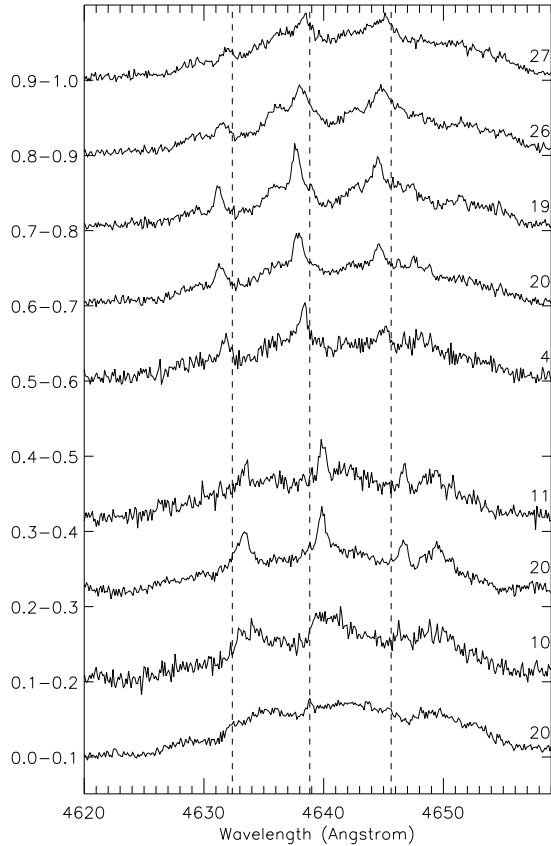


**Figure 2.** Averaged spectra from the 2011 June WHT observations of Sco X-1, plotted as a function of orbital phase. Each plotted spectrum is the average of all those observed in the phase range listed on the  $y$ -axis. The number of individual spectra comprising each plotted spectrum is shown against the right-hand  $y$ -axis. The spectra have been scaled and offset vertically to illustrate the changing strength of the Bowen lines. The dashed lines show the (system) rest-frame wavelengths for the Bowen lines, shifted by the systemic velocity  $\gamma$  (Table 2). Note that no spectra were observed with WHT in the phase range 0.4–0.5 in 2011.

### 3.2. Bowen blend spectroscopy

The earlier measurement of the orbital period of Sco X-1 (Gottlieb et al. 1975) was based on such a long baseline (84.8 yr) that we did not initially anticipate being able to improve on the precision. Our optical spectroscopic data were limited to a much shorter timespan, just 12 yr. However, the precision of the orbital period measurement also depends on how precisely the orbital phase can be measured at any epoch. For the photometric data, the phasing is rather poor, due to the low measurement precision and the intrinsic photometric variability. On the other hand, the results of SC02 suggest that for a few days of radial velocity measurements, the orbital phase can be measured to approximately  $\Delta T_0 = 0.003$  d, or 0.4%. Assuming we could make an equally good measurement from our new data, the achievable precision can be estimated as  $\Delta P_{\text{orb}} \approx \sqrt{2(\Delta T_0)^2/n_{\text{cyc}}}$ , where  $n_{\text{cyc}}$  is the number of orbital cycles between the two measurements. Our WHT observations in 2011 June were approximately 5550 cycles after those of 1999 July, suggesting an achievable precision of  $\Delta P_{\text{orb}} \approx 7 \times 10^{-7}$  d. This precision is 30% better than that quoted by Gottlieb et al. (1975), motivating a combined analysis of the two datasets.

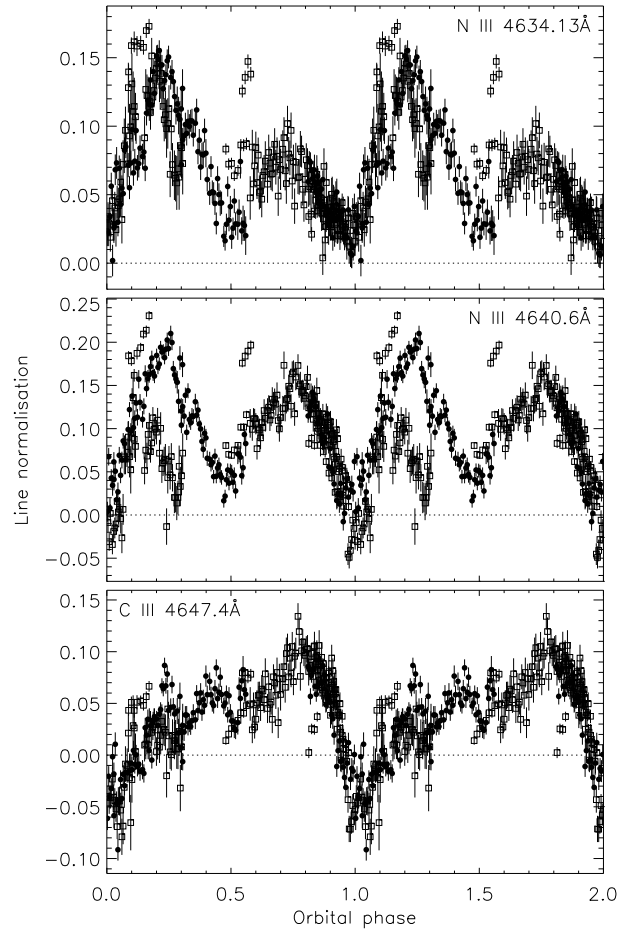


**Figure 3.** Best-fit normalisation (relative to the continuum) for each of the Bowen lines (4634.13 Å, 4640.6 Å and 4647.4 Å) in Sco X-1, from the 1999 and 2011 WHT observation epochs. The 1999 observations are shown as filled circles, while the 2011 observations are shown as open squares. Two cycles are shown in each panel for clarity. Note the marked difference in the line strength both between and within the two main observing epochs, particularly for the NIII 4640.6 Å line within phase ranges 0.1–0.3 and 0.5–0.6.

We first examined the WHT spectra to determine the properties of the Bowen lines. We show the spectrum within the wavelength range of interest, grouped and averaged within orbital phase bins of width  $\Delta\phi = 0.1$  (according to the ephemeris of SC02), in Figure 2. The lines are strong and clearly visible in the phase range 0.1–0.9, but become weak around phase zero. At this phase, we face the unirradiated side of the secondary, also corresponding to the phase of minimum light. It is thus not unexpected that the strength of the emission lines is weakest at this phase compared to other phases.

We examined the fitted normalisation for each of the lines individually in Fig. 3. The intensity of the 4634.13 Å and 4640.6 Å (NIII) lines show a marked double-peaked variation, with the maximum at phase 0.25, and primary and secondary minima at phase 0.0 and 0.5, respectively. In contrast, there was no secondary minimum for the 4647.4 Å (CIII) line intensity, which was also the weakest of the three. The best-fit normalisation exhibited an asymmetry opposite in sense to the NIII lines, reaching a maximum at around phase 0.8. These lightcurves

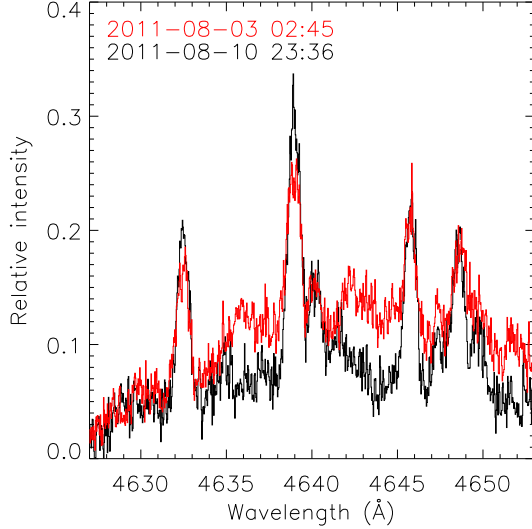


**Figure 4.** Example VLT spectra showing significant variations in Bowen line strength on timescales of a week. The spectra shown were observed by the VLT in 2011, on Aug 3 (orbital phase  $\phi = 0.570$ ) and Aug 10 ( $\phi = 0.565$ ). Note the dramatic difference in the strength of the lines between the two spectra, despite the closeness in time and orbital phase.

differ substantially from the single peak at phase 0.5 expected for uniform illumination of the front face of the donor’s Roche lobe. It seems plausible that some of the structure in our lightcurves may be caused by systematic errors introduced by the (sometimes poorly constrained) broad component underlying the Bowen lines. However, inspection of the trailed spectra appears to confirm that the strong peak at phase 0.25 is real, as is the (weaker) peak at 0.75. Taking the lightcurves at face value, it appears that the emission may not be symmetric around the  $L_1$  point, with both sides contributing, and the side away from the gas stream brightest.

Further clouding the pattern of line intensity variability was evidence for epoch-to-epoch variations. For the 4640.6Å (NIII) line (Fig. 3, middle panel), the relative normalisation measured by WHT around phase 0.2 in 2011 was significantly lower than in 1999. All these data were taken on the same night, which might suggest that a calibration issue present only on that night gave rise to the lower intensities. However, the best-fit normalisation for the other two lines measured on that night are more consistent between epochs. Furthermore, VLT data taken in an overlapping phase range just one month later shows significantly *higher* intensity for this line. This is also seen between phase 0.5–0.6, when VLT measurements taken at two epochs (in 2011 August, separated by just 8 days) exhibit intensities that vary by approximately 55%, far in excess of the estimated uncertainty. This is illustrated in the example spectra plotted in Fig. 4. These variations are thus intrinsic to the source and suggest changes in the emission line regions occur on non-orbital timescales.

The weakness of the lines around phase 0 had a dramatic effect on the radial velocity fits. We show in Figure 5 the fitted radial velocities for the combined 1999 and 2011 data. The measurements deviate very significantly from the predicted values near the phase range 0.9–1.0 and 0.0–0.1. Within these phase ranges, the narrow com-

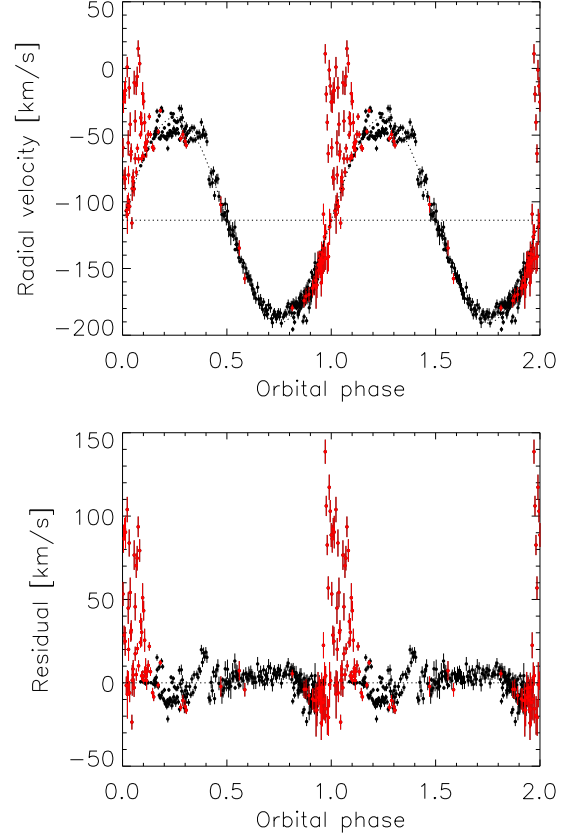


**Figure 5.** Radial velocities for Sco X-1 determined from the 1999 and 2011 WHT data, and 2011 VLT measurements. In the upper panel we show the radial velocities with the orbital model of SC02 overlotted as a dotted sinusoid. The systemic velocity is also shown as a horizontal dotted line. The points are coloured according to the minimum significance of the line detection,  $S_{\min}$  (see text). Measurements with  $S_{\min} \leq 2$  are shown in red, while those with  $S_{\min} > 2$  are plotted as black. The data are plotted twice for clarity. The lower panel shows the residuals once the model is subtracted. Note the very significant residuals around phase zero. Error bars indicate the statistical  $1\text{-}\sigma$  uncertainty.

ponents were much weaker than at other phases, leading to unreliable radial velocity measurements. Similar deviations were present in the original analysis of the 1999 data (see Fig. 3 of SC02), although nowhere near as large. Here the higher spectral resolution for the 2011 data may have led to a lower signal-to-noise for the weak lines in any given bin. However, we repeated our radial-velocity measurements with the 2011 spectra rebinned to the same resolution as the 1999 observations, and found no reduction of the systematic errors. Thus, it may instead be the lower line intensity measured in 2011 that played the main role in determining the systematic errors.

We screened the data to eliminate those unreliable velocities, by calculating the minimum detection significance for three lines. For each line  $i$ , we estimate the significance as  $A_i/\sigma_i$ , where  $A_i$  is the fitted line normalisation and  $\sigma_i$  the uncertainty (recall that the line width is fixed). We calculated

$$S_{\min} = \min(A_1/\sigma_1, A_2/\sigma_2, A_3/\sigma_3) \quad (2)$$

and rejected any measurements with  $S_{\min} \leq 2$  (plotted in red in Fig. 5). In this manner, we identified 96 of the

338 WHT & VLT measurements as unreliable.

We fitted the remaining 242 measurements with a sinusoid, offset by the systemic velocity,  $\gamma$ . We varied the input  $T_0$  value to obtain the smallest possible cross-term in the covariance matrix between  $T_0$  and  $P_{\text{orb}}$  (see below). We obtained a best-fit reduced- $\chi^2$  value of 8.5 for 238 degrees of freedom (DOF). The high  $\chi^2$  indicates that systematic errors are still likely present at a significant level, and so we scaled the measurement errors by  $\sqrt{8.5}$  in order to obtain a reduced  $\chi^2_{\nu} = 1.0$  and estimate conservative parameter uncertainties. We obtained the following system parameters

$$\begin{aligned}\gamma &= -113.8 \pm 0.5 \text{ km s}^{-1} \\ K &= 74.9 \pm 0.5 \text{ km s}^{-1} \\ T_0 &= 2454635.3683 \pm 0.0012 \text{ (HJD)} \\ P_{\text{orb}} &= 0.7873114 \pm 0.0000005 \text{ d}\end{aligned}$$

where the uncertainties (here and throughout) are at the 1- $\sigma$  (68%) confidence level. Rescaling the uncertainties in this way implicitly assumes that the uncertainties are systematically underestimated. However, here there is likely also a contribution of purely systematic errors, which should instead be added in quadrature to the measurement uncertainties. To estimate the upper limit of such a contribution, we introduced such a systematic contribution and varied the magnitude until we again reached a reduced  $\chi^2$  of approximately 1. The required contribution was  $6.2 \text{ km s}^{-1}$ ; the resulting fit parameters were consistent with those obtained by simply rescaling the errors, to within  $\approx 1\sigma$ .

The precision of  $P_{\text{orb}}$  has been improved by approximately 50%, more than expected given our initial predictions. This is likely due to the addition of the VLT data, which offers slightly better radial velocity precision; the average (statistical) uncertainty for the VLT measurements for which the line significance was above the threshold was  $2.2 \text{ km s}^{-1}$ , compared to  $3.2 \text{ km s}^{-1}$  for WHT. The new value is discrepant with that of Gottlieb et al. (1975) at only the  $1.3\sigma$  level.

The systemic velocity  $\gamma$  is also consistent to within the uncertainties with the previous value of SC02. However, the velocity amplitude  $K$  is significantly ( $4.4\sigma$ ) lower. We initially attributed this discrepancy to the screening of the radial velocity measurements. The systematic uncertainties contributed by the weakness of the spectral lines around phase zero tended to result in radial velocities significantly higher than predictions. Together, these systematic errors could be expected to bias the velocity amplitude to higher values (as well as potentially shifting the  $T_0$  earlier). To test this hypothesis, we performed radial velocity fits to the 1999 observations alone, with the orbital period fixed at the Gottlieb et al. (1975) value (essentially replicating the analysis of SC02). The velocity amplitude without (with) screening was  $77.2 \pm 0.4 \text{ km s}^{-1}$  ( $76.4 \pm 0.3 \text{ km s}^{-1}$ ). While the amplitude obtained using all the 1999 measurements was identical to the analysis of SC02, the value adopting the screening criteria was discrepant at less than the  $2\sigma$  level. Thus, it seems likely that the discrepancy between the best-fit velocity amplitude for the combined data and the results of SC02 is instead related to a change in the geometry of the line emission region between epochs.

To compare the newly-derived  $T_0$  with that of SC02, we subtracted an integer number of orbital cycles (4162) to give fractional days 0.5783 compared to 0.568. Again, the discrepancy is significant ( $3.2\sigma$ , not taking into account the contribution of the projected uncertainty on  $P_{\text{orb}}$ ) but the sense is in the direction that we expect from the known radial velocity bias around phase zero. Thus, we expect that our new  $T_0$  is more reliable than that of SC02, although systematic uncertainties arising from changes in the emission geometry from epoch to epoch may yet contribute to this discrepancy.

Similarly, we subtracted 1429 orbital cycles to compare with the ephemeris of Hynes & Britt (2012). We obtain fractional days of 0.3003 compared to 0.329, which is consistent (at the  $1.7\sigma$  level). The relative phasing of the photometric minimum  $T_{\text{min}}$  is  $0.039 \pm 0.017$ , which is also consistent with the relative phasing of the Gottlieb et al. (1975) data as calculated by SC02.

The best-fit orbital parameters are listed in Table 2, along with the epoch of inferior conjunction  $T_0$  in units of GPS seconds<sup>7</sup>. We also quote the off-diagonal term from the covariance matrix  $V(P_{\text{orb}}, T_0)$  giving the cross-term between  $P_{\text{orb}}$  and  $T_0$ , critical for determining the propagated error on the future epoch of inferior conjunction. We caution that the measured velocity amplitude  $K$  is likely an underestimate of the velocity amplitude of the companion's centre of mass, as the line emission is dominated by the heated face of the companion (e.g. Muñoz-Darias et al. 2005). We also defer any attempt to refine the projected velocity of the neutron star itself.

One additional systematic uncertainty that must be considered arises from the possibility that the centre of light for the Bowen lines does not lie on the line joining the centres of mass of the two stars. Such a situation might arise from asymmetries in the accretion stream or impact point, leading to differential illumination on the leading compared to the trailing side of the donor. In that case, the true inferior conjunction would occur earlier or later compared to the epoch inferred from the Bowen line spectroscopy. Since the distribution of emission across the donor is unknown, and is likely variable on non-orbital timescales, it is not currently feasible to construct a detailed model. Instead we derive here some limits on the effect of such an emission asymmetry on the ephemeris. Firstly, we note that the system parameters most consistent with the spectroscopic measurements and the inferred system inclination have mass ratio  $q \approx 0.3$  and  $K_2 \approx 120 \text{ km s}^{-1}$ . With the measured  $K$ -amplitude for the Bowen lines much smaller, at  $75 \text{ km s}^{-1}$ , the emission region must be close to the  $L_1$  point. The angular size of the region on the donor with this velocity is approximately  $8^\circ$ . Secondly, the degree of the asymmetry on the donor is restricted by the relative emission at different phases. Since we see emission at both phase 0.25 and 0.75, the line emission cannot arise from one side alone; with a typical contrast of 50% between the line amplitudes at these phases, the maximum shift is likely no more than half of the region's angular size, or  $\pm 2^\circ$ . This corresponds to a phase error of

<sup>7</sup> GPS time zero is 1980 Jan 6 00:00 UT (JD 2444244.5), and since it is not perturbed by leap seconds is now ahead of UTC by 16 seconds as of 2012 July 1 — see <http://hpiers.obspm.fr/iers/bul/bulc/bulletinc.dat>

**Table 2**  
Orbital parameters for Sco X-1 derived from multi-epoch fits to radial-velocity measurements

Parameter	Value	Units.
$\gamma$	$-113.8 \pm 0.5$	$\text{km s}^{-1}$
$K$	$74.9 \pm 0.5$	$\text{km s}^{-1}$
$T_0$	$2454635.3683 \pm 0.0012$	HJD
	$897771000 \pm 100$	GPS seconds
$P_{\text{orb}}$	2008 June 17 at 20:50:00	UTC
	$0.7873114 \pm 0.0000005$	d
$ V(P_{\text{orb}}, T_0) $	$3.614 \times 10^{-11}$	$\text{d}^2$

0.005 d, or approximately 4 times the (statistical) error attributed to  $T_0$  (Table 2).

### 3.3. Parameters for future GW searches

Here we establish the orbital parameters and uncertainties likely to apply for future searches for gravitational waves. The current scenario for the operation of the Advanced LIGO-Virgo (aLIGO) network over the next decade involves a series of commissioning periods with increasing sensitivity beginning in 2015, leading to the operation of the full network with full sensitivity by 2019 (LIGO Scientific Collaboration et al. 2013).

We note that the orbital phase for  $T_0$  corresponds to inferior conjunction of the mass donor, that is, at  $T_0$  the companion is closest to Earth, and the compact object is at its most distant. If the quoted orbital parameters are to be used for searches for gravitational waves, the relative phasing should be taken into account, and an offset of  $0.5P_{\text{orb}}$  added to the reference phase if necessary (depending on the expression for the orbital motion).

In the absence of significant orbital period evolution, the orbital period uncertainty measured here is the correct value to use for future searches. However, the correct  $T_0$  uncertainty at a future epoch will depend on the time elapsed since the measurement, as well as the uncertainties on both  $T_0$  and  $P_{\text{orb}}$ . We here describe how the error on  $T_0$  may be projected in time to any given epoch. The epoch for inferior conjunction  $T_n$  is given by

$$T_n = nP_{\text{orb}} + T_0 \quad (3)$$

where  $P_{\text{orb}}$  and  $T_0$  are given in Table 2 and  $n$  is an integer. The uncertainty  $\sigma_n$  is thus

$$\sigma_n^2 = \left( \frac{\partial T_n}{\partial P_{\text{orb}}} \right)^2 \sigma_{P_{\text{orb}}}^2 + \left( \frac{\partial T_n}{\partial T_0} \right)^2 \sigma_{T_0}^2 + 2 \left( \frac{\partial T_n}{\partial P_{\text{orb}}} \frac{\partial T_n}{\partial T_0} \right) V(P_{\text{orb}}, T_0) \quad (4)$$

$$= n^2 \sigma_{P_{\text{orb}}}^2 + \sigma_{T_0}^2 + 2nV(P_{\text{orb}}, T_0) \quad (5)$$

where  $\sigma_{P_{\text{orb}}}$  and  $\sigma_{T_0}$  are the uncertainties in  $P_{\text{orb}}$  and  $T_0$  respectively, and  $V(P_{\text{orb}}, T_0)$  is the cross-term of the covariance matrix (from Table 2). Substituting in the values from Table 2, we express the error in  $T_n$  as

$$\sigma_{0,t} \approx [3.9 \times 10^{-13}(t/1 \text{ d})^2 + 9.2 \times 10^{-11}(t/1 \text{ d}) + 1.4 \times 10^{-6}]^{1/2} \text{ d} \quad (6)$$

$$= [5.3 \times 10^{-8}(t/1 \text{ yr})^2 + 3.4 \times 10^{-8}(t/1 \text{ yr}) + 1.4 \times 10^{-6}]^{1/2} \text{ d} \quad (7)$$

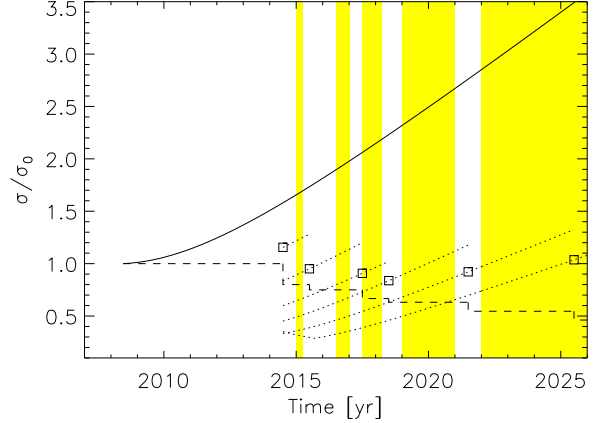


**Figure 6.** The projected uncertainty in the epoch of inferior conjunction  $T_0$  (solid line) throughout the aLIGO observing intervals (shaded bands). Note the approximately linear growth of the effective error throughout the aLIGO commissioning and observing period (2015–), in the absence of additional epochs of optical observations. The approximate effect of additional observing epochs (open squares) is shown on the  $T_0$  uncertainty (dotted curves) and the orbital period  $P_{\text{orb}}$  (dashed line).

where  $\sigma_{0,t}$  is the uncertainty in the epoch of inferior conjunction at time  $t$  in days since  $T_0$ . The magnitude of  $\sigma_{0,t}$  is rapidly dominated by the  $\sigma_{P_{\text{orb}}}$  term, and at late times will grow linearly due primarily to this factor, as  $\sigma_{0,t} \propto n\sigma_{P_{\text{orb}}} \approx 2.1 \times 10^{-4} (t/1 \text{ yr}) \text{ d}$ . We show the evolution of  $\sigma_{0,t}$  (i.e. the size of the parameter space that must be spanned by the search) as a function of time in Figure 6. From 2015, the effective uncertainty will grow approximately linearly with time, doubling by 2017 and exceeding  $3\times$  the current error level by the time that full-network observations commence sometime after 2022. Although this is less than ideal, we point out that even with the data in hand, the ephemeris derived in this paper gives an effective uncertainty in  $T_0$  a factor of four smaller than for the previous ephemeris of SC02.

However, additional investment in observing time will help to further refine the orbital parameters, and improve the sensitivity of future searches. We have estimated the effect of additional epochs of radial velocity measurements from 2014 onwards, based on the following assumptions. First, that the uncertainty on  $P_{\text{orb}}$  decreases as  $1/\Delta T$ , where  $\Delta T$  is the total span of the observations. Our results to date indicate that this is a conservative assumption (see §3.2). Second, that the uncertainty on  $T_0$  decreases as  $1/n_{\text{obs}}$ , where  $n_{\text{obs}}$  is the total number of observations. We consider each observing epoch to consist of 3 nights of WHT observations, resulting in 100 radial velocity measurements, and neglect any rejection of data required due to systematic errors around phase zero. The resulting uncertainty curves for observations in 2014, 15, 17, 18, 21, and 24 (roughly in between each aLIGO observing epoch) are also shown in Fig. 6. A relatively modest investment in observing time (6 additional epochs, totalling 18 nights, over a decade) will allow us to maintain the  $T_0$  uncertainty at or below the current level ( $\approx 10^{-3} \text{ d}$ ) throughout the aLIGO observations. Additionally, we will incrementally improve the uncertainty on the orbital period, down to a level of approximately  $2.3 \times 10^{-7} \text{ d}$ .



## 4. DISCUSSION

From analysis of spectroscopic and photometric data taken over a 12-yr baseline, we have obtained an improved set of orbital parameters for the X-ray binary Sco X-1. ASAS photometric data supports the Gottlieb et al. (1975) orbital period over the alias suggested by Vanderlinde et al. (2003) measured from the *RXTE*/ASM data (as found by Hynes & Britt 2012). Although further improvement in the orbital parameters via photometry is unfeasible, due to large-amplitude aperiodic variations, we also obtained an additional epoch of spectroscopic measurements which resulted in an improvement in the precision of the orbital period  $P_{\text{orb}}$  (compared to that quoted by Gottlieb et al. 1975) of a factor of two. We also improved the precision of the epoch of inferior conjunction  $T_0$  (compared to that of SC02) by a factor of 2.5.

In contrast to the previous WHT/ISIS spectroscopic measurements of SC02, which were performed with a slightly lower spectral resolution (0.84 Å compared to 0.3 Å for the 2011 WHT measurements) we found substantial systematic errors in the measured radial velocities close to phase zero. We attributed these errors to the relative weakness of the lines at this phase; the unirradiated side of the companion is facing us, so that the line-emitting region is partially obscured. Most notably, we found a significant variation in the measured velocity amplitude of the Bowen lines, as well as the time of inferior conjunction compared to the earlier ephemeris. These variations do not seem to be related to the systematic uncertainties contributed to the weakness of the lines around inferior conjunction, but instead likely indicate a change in the emission geometry between epochs. Variations in the Bowen line intensities on timescales as short as 1 week offer further evidence for alterations to the emission pattern. We also estimate that possible anisotropy of the emission with respect to the line joining the centres of mass of the two objects, may contribute a systematic error in the epoch of inferior conjunction of 0.005 d, or approximately 4 times the statistical uncertainty from the spectral line fitting. It is hoped that additional spectroscopic data resolving the emission, together with a more detailed model of the emission geometry, will improve constraints on this contribution.

We also considered the impact of the system parameters on future gravitational wave searches, as planned with aLIGO. Watts et al. (2008) quantified the search sensitivity via the number of model templates required to cover the parameter space defined by the uncertainties in each of the orbital parameters. The number of templates required for each parameter depends linearly on the parameter uncertainty, but because correlations between the parameters can be important, the number of templates for a joint subspace is not equal to simply the product of the number of templates for each parameter individually. That is, the number of templates for a joint search of  $P_{\text{orb}}, T_0$  space is

$$N_{P_{\text{orb}}, T_0} \propto \Delta[P_{\text{orb}}^{-2}] \Delta[T_0] \quad (8)$$

where  $\Delta[\lambda^i] = \lambda_{\text{max}}^i - \lambda_{\text{min}}^i$  for parameter  $\lambda^i$ . Based on this proportionality, we can quantify the expected improvement in sensitivity based on the fractional reduction in the number of templates arising from the reduction in

uncertainty in each parameter. This is a factor of 5 for the parameters listed in Table 2.

However, this factor only approximately represents the improvement in sensitivity achieved for future gravitational wave searches using the orbital parameters determined in this paper, because the effective uncertainty in the orbital parameters (particularly  $T_0$ ) at the epoch of future searches must be calculated including the contributions from the other parameters. With the results from this analysis, we expect the improvement in the  $T_0$  uncertainty from 2015 onwards, when aLIGO observations commence, at a factor of 4 or better, giving an overall improvement of a factor of 10 in the number of templates. Additionally, we demonstrate in section §3.3 that a modest investment in optical observing time over the next decade can result in an improvement likely of a factor of 50. We point out that this is a conservative estimate, and we expect to improve considerably on this prediction, based on a number of additional efforts, detailed below.

First, based on the results from our 2011 pilot observations, we will refine our observing strategy to optimise our radial velocity measurements. This will likely involve longer integration times for spectra, but we will also request scheduling of our future observations to avoid the times around phase zero. Second, we plan to exploit other observing campaigns (such as the program by which we obtained the VLT data in 2011) which can provide radial velocity measurements with smaller uncertainties than the WHT data. Third, we will investigate the emission line morphology via Doppler tomography, to obtain an improved estimate of  $a_x \sin i$ , over that of SC02. Fourth, we will investigate complementary modelling efforts that can allow us to refine our radial velocity measurements, based on inferences of the emission pattern on the surface of the companion. Fifth, we have an on-going program to carry out an X-ray pulsation search of extensive archival *Rossi X-ray Timing Explorer* data of Sco X-1. Improvements in the orbital ephemeris, as we have presented here, offer improved sensitivity for X-ray pulsation searches, in an analogous manner to gravitational wave searches. Although the pulsations and orbital variations are effectively decoupled (e.g Watts et al. 2008), the lack of knowledge of the spin frequency of this source contributes the largest share of the number of templates for the gravitational wave search. Thus, detection of pulsations in this system, as well as being a first for a Z-source, and a conclusive verification of the neutron-star nature of the object, would offer the most substantial improvement in the search sensitivity of any of the work presented here.

We are grateful to Stuart Littlefair who traded 3 hours of observing time on the WHT to improve our coverage of the Sco X-1 orbit in 2011. We thank the anonymous referee for their feedback, which significantly improved this paper. This project was supported in part by the Monash-Warwick Strategic Funding Initiative. DKG is the recipient of an Australian Research Council Future Fellowship (project FT0991598). DS acknowledges support from STFC through an Advanced Fellowship (PP/D005914/1) as well as grant ST/I001719/1. JC acknowledges the support of the Spanish Ministerio



de Economía y Competitividad (MINECO) under grant AYA2010–18080. RC acknowledges a Ramon y Cajal fellowship (RYC-2007-01046). This research was carried out using the PAMELA and MOLLY software packages, written by Tom Marsh (Warwick), and also made use of the SIMBAD database, operated at CDS, Strasbourg, France.

Facilities: WHT, VLT.

#### REFERENCES

- Abbott, B., Abbott, R., Adhikari, R., Agresti, J., Ajith, P., Allen, B., Amin, R., Anderson, S. B., Anderson, W. G., Arain, M., & et al. 2007, *Phys. Rev. D*, 76, 082003
- Abbott, B. e. a. L. 2007, *Phys. Rev. D*, 76, 082001
- Bildsten, L. 1998, *ApJ*, 501, L89
- Chakrabarty, D., Morgan, E. H., Munro, M. P., Galloway, D. K., Wijnands, R., van der Klis, M., & Markwardt, C. B. 2003, *Nature*, 424, 42
- Chung, C. T. Y., Melatos, A., Krishnan, B., & Whelan, J. T. 2011, *MNRAS*, 414, 2650
- Dekker, H., D’Odorico, S., Kaufer, A., Delabre, B., & Kotzlowski, H. 2000, in *Society of Photo-Optical Instrumentation Engineers (SPIE) Conference Series*, Vol. 4008, Society of Photo-Optical Instrumentation Engineers (SPIE) Conference Series, ed. M. Iye & A. F. Moorwood, 534–545
- Dhurandhar, S., Krishnan, B., Mukhopadhyay, H., & Whelan, J. T. 2008, *Phys. Rev. D*, 77, 082001
- Gottlieb, E. W., Wright, E. L., & Liller, W. 1975, *ApJ*, 195, L33
- Hasinger, G. & van der Klis, M. 1989, *A&A*, 225, 79
- Hynes, R. I. & Britt, C. T. 2012, *ApJ*, 755, 66
- LIGO Scientific Collaboration, Virgo Collaboration, Aasi, J., Abadie, J., Abbott, B. P., Abbott, R., Abbott, T. D., Abernathy, M., Accadia, T., Acernese, F., & et al. 2013, *ArXiv e-prints* 1304.0670v1
- Muñoz-Darias, T., Casares, J., & Martínez-Pais, I. G. 2005, *ApJ*, 635, 502
- Oke, J. B. 1990, *AJ*, 99, 1621
- Pojmanski, G. & Maciejewski, G. 2004, *AcA*, 54, 153
- Steeghs, D. & Casares, J. 2002, *ApJ*, 568, 273
- Vanderlinde, K. W., Levine, A. M., & Rappaport, S. A. 2003, *PASP*, 115, 739
- Watts, A. L. 2012, *ARA&A*, 50, 609
- Watts, A. L., Krishnan, B., Bildsten, L., & Schutz, B. F. 2008, *MNRAS*, 389, 839